Communication—Binder Effects on Cycling Performance of High Areal Capacity SPAN Electrodes

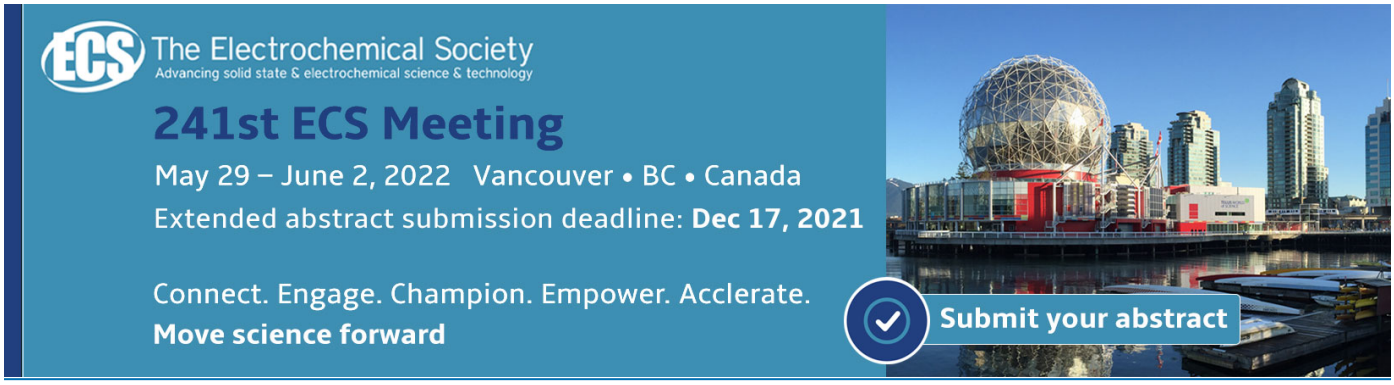

Journal of The Electrochemical Society, 2021 **168** 110504
1945-7111/2021/168(11)/110504/5/$40.00 © 2021 The Electrochemical Society ("ECS"). Published on behalf of ECS by IOP Publishing Limited

Communication—Binder Effects on Cycling Performance of High Areal Capacity SPAN Electrodes

Zhaohui Wu,[1,2] Haodong Liu,[2] Sicen Yu,[2,3] and Ping Liu[1,2,3,*,z]

[1]*Program of Chemical Engineering, University of California San Diego, La Jolla, California 92093, United States of America*
[2]*Department of Nano Engineering, University of California San Diego, La Jolla, California 92093, United States of America*
[3]*Program of Materials Science, University of California San Diego, La Jolla, California 92093, United States of America*

We report here the binder effect on the cycling performance of high areal capacity sulfurized polyacrylonitrile (SPAN) cathodes (>6 mAh cm^{-2}). Thick SPAN cathode with the polyvinylidene difluoride (PVdF) binder only maintains 66.7% capacity at 60th cycle. Mechanical integrity failure is responsible for the decay indicated by morphological and mechanical analysis. Carboxymethylcellulose (CMC) markably improves the corresponding capacity retention to 94.5%. Stable cycling of low porosity (30%) cathode is also enabled by binder optimization. This work shows the importance of binder choice on thick SPAN cathodes and paves the way for high energy density Li||SPAN cell.
 [DOI: 10.1149/1945-7111/ac315b]

Manuscript submitted August 3, 2021; revised manuscript received September 18, 2021. Published November 2, 2021.

Supplementary material for this article is available online

Li-S battery is regarded as a highly desirable choice to replace Li-ion batteries due to its high energy density and the absence of transition metals. Sulfurized polyacrylonitrile (SPAN) has promising specific energy (>1249 Wh kg^{-1}) with superior cycling performance, in contrast to elemental S-based materials.[1,2] In addition, the solid-solid reaction mechanism of SPAN unlocks the possibility of decreasing the porosity of the electrode, key to minimizing the amount of electrolyte and achieve high cell energy density.[3] However, most reported studies on SPAN have been performed with modest active material loadings, resulting in low practical cell-level energy densities.[4–6] The main challenges for high loading cathodes are mechanical failures such as cracking and delamination from the current collector, leading to cell capacity degradation as the conductive network breaks. These structure failures are further exaggerated by the volume change during repeated lithiation and de-lithiation.[7] To address these challenges, binder is the key as they provide the mechanical skeleton of the electrode structure. Regarding the amount of binder, 10% is commonly used in literature to fabricate SPAN electrodes.[6,8,9] Adding more binder could improve the durability of the SPAN cathode but sacrifice the overall energy density. Improving the mechanical property of the binder is another way to tackle this problem without sacrifing cell energy. For example, Yang et al. and Chen et al. have developed two novel binders to improve the cycling performance of SPAN cathode.[7,10] However, their binders are not commercially available, which limit their practical applications.

This work studies the effects of binders on the cycling performance of high areal capacity (>6 mAh g^{-1}) SPAN cathode. We compare electrodes made with two commercially available binders, PVdF and CMC. Although previous work indicates that CMC binder improves the rate capability of SPAN electrodes with low areal capacity (~1 mAh cm^{-2}),[11] here, we show that the choice of the binder has a decisive effect on the mechanical integrity and cycling stability of high areal capacity SPAN cathodes, especially at low electrode porosities.

Experimental

The synthesis of SPAN was described previously.[12] The electrodes were made by mixing SPAN, SuperP, and binder (PVdF or CMC) in an 8:1:1 ratio. After drying, electrodes were punched into 12 mm disks. Roll-press calendering was employed to control the porosity of the cathode. The thickness of the electrode was measured by a micrometer to confirm that the desired porosity was achieved. The porosity of the electrode is calculated by the following equation:

$$\in = \left(1 - \frac{\rho_{appa}}{\rho_{theo}}\right) \times 100\%$$

$$= \left(1 - \frac{\frac{W_{cathode}}{V_{cathode}}}{\rho_{SPAN} \times u_{SPAN} + \rho_{carbon} \times u_{carbon} + \rho_{binder} \times u_{binder}}\right) \times 100\%$$

where ρ_{appa}, ρ_{theo}, $W_{cathode}$, $V_{cathode}$, ρ_{span}, u_{span}, ρ_{carbon}, u_{carbon}, ρ_{binder}, u_{binder}, are the apparent density, theoretical density, weight, and volume of the cathode; density, and volume fraction of SPAN; density, and volume fraction of carbon, density, and volume fraction of binder, respectively. The densities of the active material, carbon black, and binder used for porosity calculation were 1.81, 2.0, and 1.78 or 1.6 g cm^{-3}, respectively. 2032 coin cells were assembled in argon filled glovebox with oxgen and moisture levels of <0.1 ppm. The electrolyte was prepared by mixing 1.8 M LiFSI in Diethyl ether (DEE)/Bis(2,2,2-trifluoroethyl)ether (BTFE) (weight ratio 1:4) solution. Cells were cycled at C/20 rate for two cycles and then switched to C/5 rate. Electrochemical impedance spectroscopy (EIS) was performed using BioLogic VSP 300 potentiostat from 7 MHz to 10 mHz. Scanning electron microscopy (SEM) was performed on the FEI Quanta 250 SEM. The 180° peeling test was adopted from work by Ryou et al.[13]

Results and Discussion

We first performed a cell specific energy modeling to define the desired cathode loading. As shown in Fig. S1 (available online at stacks.iop.org/JES/168/110504/mmedia), a loading of >6 mAh cm^{-2} is required to reach 334 Wh kg^{-1} for the Li||SPAN cell, enough to compete with Li-ion batteries.[14] When PVdF is used as the binder, the SPAN electrode with a 1 mg cm^{-2} loading and 50% porosity shows excellent cycling stability, with no noticeable change of the voltage profiles throughout 60 cycles at a C/5 rate, indicating the material itself is highly stable (Figs. 1a and 1b). We chose a rate of C/5 for cycling since it is close to practical battery operation conditions. Even higher rates would lead to severe degradation of the lithium counter electrode due to the high current density, particularly when the cathode loading is high. Unfortunately, as shown in Figs. 1a and 1c, the Li||SPAN cell shows rapid capacity fade from 650 to 400 mAh g^{-1} within 60 cycles for an electrode loading of 10 mg cm^{-2}. The

*Electrochemical Society Member.
[z]E-mail: piliu@eng.ucsd.edu

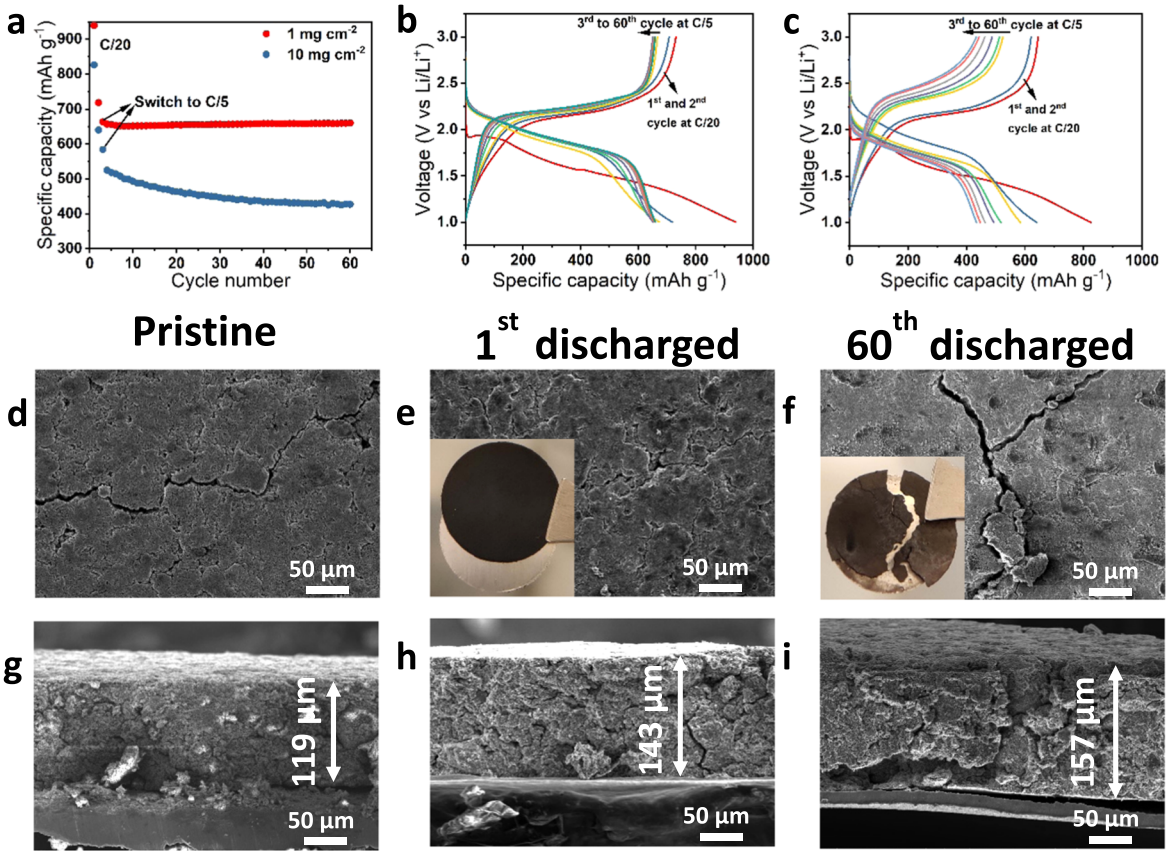

Figure 1. Comparison of the cycling performance of SPAN cathodes with different areal mass loading. (a) capacity retention of 1 mg cm^{-2} and 10 mg cm^{-2} SPAN electrode with PVdF as the binder, (b) voltage profiles of 1 mg cm^{-2} SPAN cathode, (c) voltage profiles of 10 mg cm^{-2} SPAN cathode. The cell was cycled under C/20 rate for two formation cycles and then cycled under C/5 rate, 1C = 550 mA h g^{-1}. Top view SEM images of (d) pristine, (e) 1st discharged, (f) 60th discharged high areal capacity SPAN electrode. Cross-sectional view SEM images of (g) pristine, (h) 1st discharged, (i) 60th discharged high areal capacity SPAN electrode.

corresponding voltage profiles in Fig. 1c also indicate a fast polarization increase.

The degradation observed in Fig. 1c is due to the failure of the thick cathode, not the Li anode. To prove this, we note that the electrolyte used in these tests is LDEE (1.8 M LiFSI in DEE/BTFE).[15] The average Li metal coulombic efficiency in this electrolyte is >99% for 200 cycles, in contrast to <90% with rapid deterioration in 30 cycles in carbonate electrolytes (Fig. S2). It is well known that the effect of Li degradation is insignificant at low current densities. Therefore, SPAN cathodes have been reported to be stable in carbonate electrolytes when tested against Li.[16–18] However, at high loadings and current densities, Li metal degradation becomes significant.[19,20] Figure S3 shows that Li||SPAN cell experiences continuous capacity decay in carbonate electrolytes caused by both cathode and anode failure. The use of the LDEE electrolyte thus allows us to focus on the degradation of the thick cathode only.

The morphology of the thick SPAN cathodes before and after cycling were studied by SEM. Figures 1d and 1g are the top and cross-sectional view images of the pristine cathode. The presence of

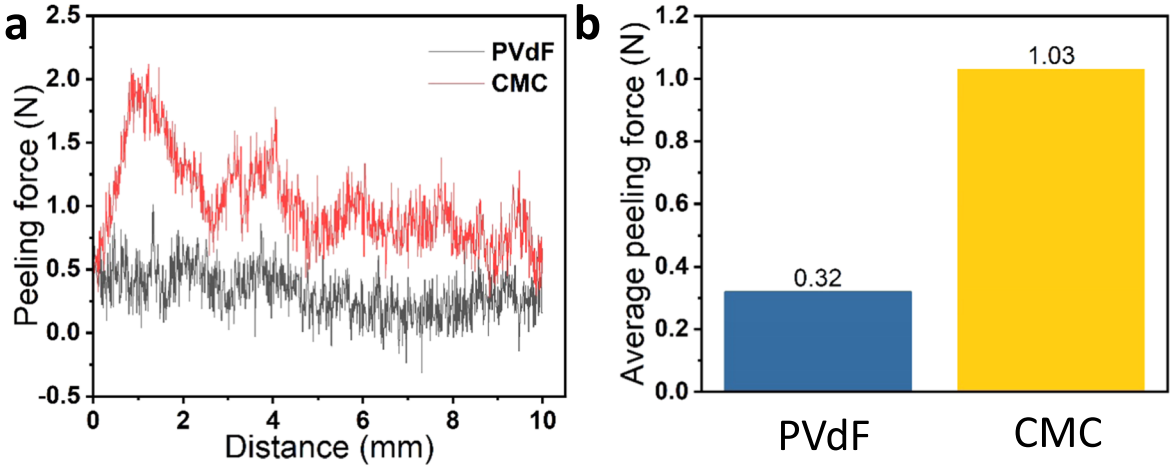

Figure 2. (a) Peeling force of 10 mg cm^{-2} SPAN electrode with different binders. (b) average peeling force.

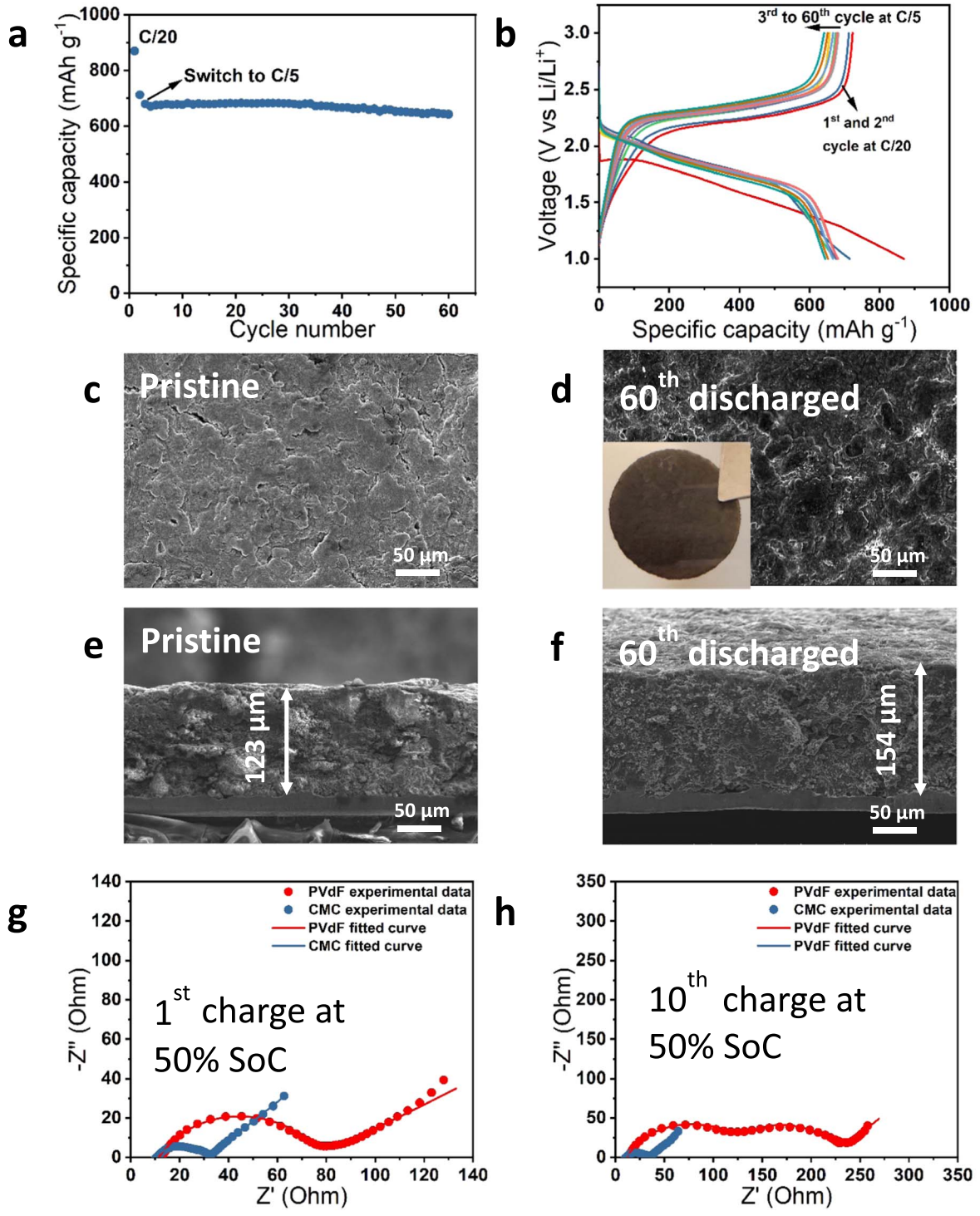

Figure 3. (a) Capacity retention of 10 mg cm^{-2} SPAN electrode with CMC as the binder. (b) Voltage profiles of the same SPAN cell. SEM images of high areal capacity SPAN cathode with CMC binder. Top-view images of (c) pristine, (d) after 60th discharge. Cross-sectional view images of (e) pristine, (f) after 60th discharge. Electrochemical impedance spectroscopy of SPAN electrode with different binder at (g) 50% SoC of 1st charge, (h) 10th charge.

cracks indicates the poor mechanical property and is likely due to the stress generated during solvent evaporation. After the 1st cycle, the electrode is shown to have already delaminated from the current collector (optical image, Fig. 1e inset). The cathode thickness has increased from 119 to 143 μm after the first lithiation (Fig. 1h). More cracks have formed vertically from the bottom to the top of the electrode. Additional contact resistance could arise at the interface between the current collector and the electrode. The mechanical failure due to crack, delamination, and volume change is likely the root cause of the rapid capacity fading of the 10 mg cm^{-2} SPAN electrode. After 60 cycles, the repeated expansion/contraction and the faster rate after formation cycles led to a more severe mechanical failure. (Figs. 1f and 1i). Cracks, delamination, and even pulverization are observed in both optical and SEM images. The mechanical

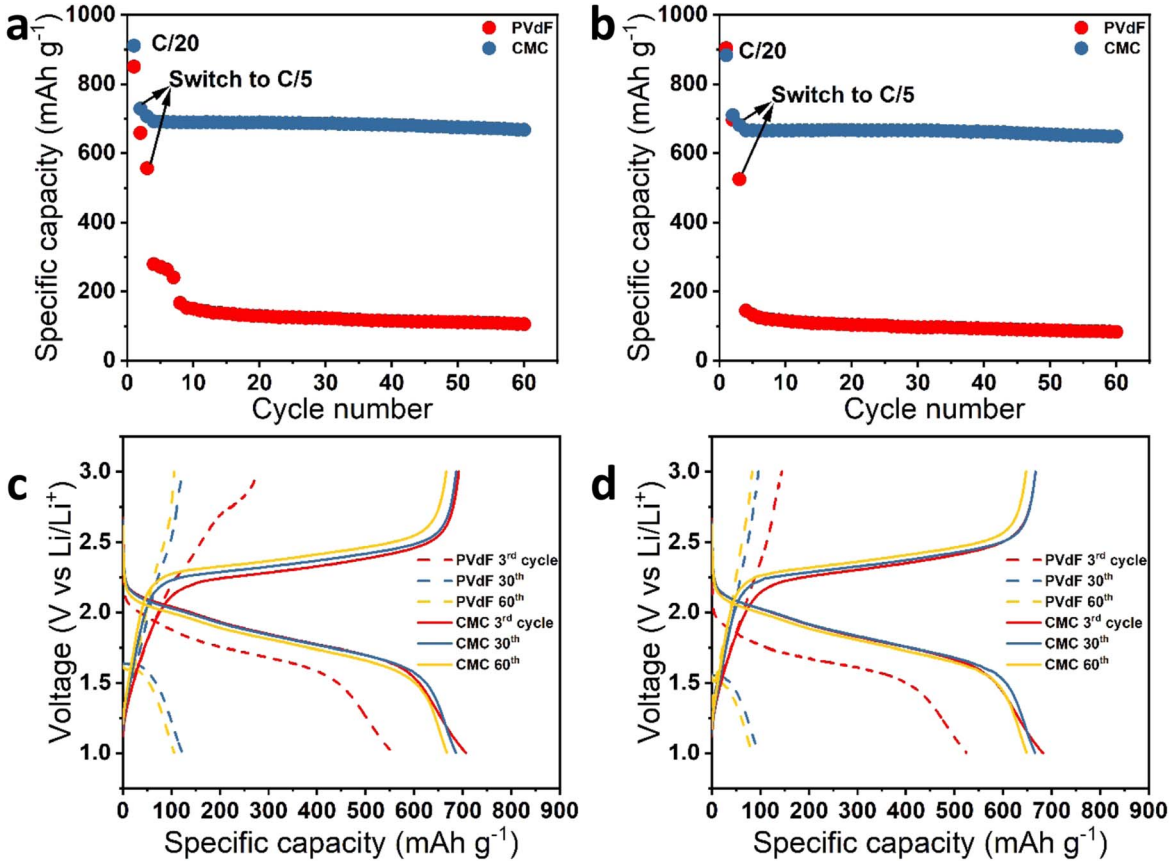

Figure 4. Comparison of the cycling performance of high areal capacity SPAN electrodes. (a) 40% cathode porosity, (b) 30% cathode porosity. Voltage profiles of Li||SPAN cells with (c) 40% cathode porosity, different binder, (d) 30% cathode porosity, different binder.

disintegration of the thick electrode will further lead to the breakage of the conductive network thus causing active material loss and/or polarization increase during cycling.

Optimizing the polymer binder is an effective approach to improve the electrode mechanical integrity. For example, He et al. showed that sulfur cathode with CMC-SBR binder performed much better than PVdF because of stronger adhesion and better dispersion.[21] Figure 2 shows the results from a 180° peeling test on thick SPAN electrodes with two different binders. The CMC-based electrode is much more robust, with an average peeling force at 1.03 N, three times that of PVDF-based electrode. As shown in Fig. 3a, the 6 mAh cm^{-2} SPAN cathode with CMC binder maintains 94.5% of its capacity (based on the 3rd cycle) at the 60th cycle, a dramatic improvement over the corresponding value of 66.7% for PVDF. The voltage profiles in Fig. 3b also indicate minimal degradation. We note that the initial reversible capacity is higher than the electrode with the PVdF binder. This is likely due to the improved mechanical property preventing SPAN particles disintegrating from the conductive network. Furthermore, the SEM images of the pristine and cycled electrodes in Figs. 3c–3f reveal no visible cracks or delamination, proving the electrode's durability. Electrochemical impedance spectroscopy (EIS) was used to characterize PVdF and CMC based electrodes after cycling. Figure 3g shows results from the electrodes at 50% SoC of the 1st charge. The EIS spectra were fitted using the equivalent circuit illustrated in Fig. S4. The much larger charge transfer resistance from the PVdF based electrode (62.68 Ω) as compared to the CMC one (21.54 Ω) implies that even after 1st discharge the cathode with PVdF binder has already degraded. The charge transfer resistance of the PVdF based electrode significantly increases to 127.4 Ω after 10 cycles, while the CMC based electrode shows only a slight increase of the cell impedance (Fig. 3h). The EIS analysis further proves the advantages of CMC binder.

Another critical step towards high energy density Li||SPAN battery is to reduce the cathode porosity. Because lower porosity electrode requires less electrolyte, resulting in higher cell level energy density. The binder plays a key role at low porosity because the SPAN electrode will expand outwardly due to the limited spaces inside, which will apply significant stress on the binder skeleton. We tested SPAN cathodes with 40% and 30% porosity, with the results shown in Figs. 4a and 4b. The capacity of PVdF based electrodes quickly decays from 600 to <150 mA h g^{-1} within 10 cycles, which is much faster than the PVdF based cathode with 50% porosity. Less room inside the electrodes promotes the outward expansion instead of inward expansion. The former leads to breakage of the carbon network, while the later could reinforce the contact between carbon and SPAN particles. Therefore, the cathode with less porosity shows a dramatically worse cyclability. In contrast, the 30% and 40% porosity SPAN electrodes using CMC binder are shown to maintain high capacity retention of 95.1% and 94.4%, respectively (Figs. 4c and 4d), clearly demonstrating the benefits of using CMC for high areal loading, low porosity SPAN cathodes.

Summary

We have studied the effect of binders on cycling performance of high areal capacity SPAN cathodes. The mechanical property of the electrode is significantly improved when switching from PVdF to CMC. Therefore, the cracking, delamination, and pulverization issues of the thick SPAN cathodes are mitigated. As a result, the SPAN cathode (>6 mAh cm^{-2}, 50% porosity) with CMC binder shows significantly improved capacity retention of 94.5% for 60 cycles, while the SPAN cathode with PVDF binder rapidly degrades to 66.7% of its original capacity. In addition, the 30% porosity electrode with CMC retains a high specific capacity of 648.6 mAh g^{-1} after 60 cycles. Thus, we show binder optimization is an essential step toward a Li||SPAN battery with high cell-level energy density.

Acknowledgments

The work was supported by the Office of Vehicle Technologies of the U.S. Department of Energy through the Advanced Battery Materials Research (BMR) Program (Battery500 Consortium) under Contract No. DE-EE0007764. Part of the work used the UCSD-MTI Battery Fabrication Facility and the UCSD-Arbin Battery Testing Facility.

ORCID

Zhaohui Wu https://orcid.org/0000-0002-1453-6784
Ping Liu https://orcid.org/0000-0002-1488-1668

References

1. J. Wang, J. Yang, J. Xie, and X. Naixin, *Adv. Mater.*, **050**, 963 (2002).
2. X. Xing, Y. Li, X. Wang, V. Petrova, H. Liu, and P. Liu, *Energy Storage Mater.*, **21**, 474 (2019).
3. J. Liu et al., *Nat. Energy*, **4**, 180 (2019).
4. Y. Z. Zhang, S. Liu, G. C. Li, G. R. Li, and X. P. Gao, *J. Mater. Chem. A*, **2**, 4652 (2014).
5. M. Frey, R. K. Zenn, S. Warneke, K. Müller, A. Hintennach, R. E. Dinnebier, and M. R. Buchmeiser, *ACS Energy Lett.*, **2**, 595 (2017).
6. X. Chen et al., *Nat. Commun.*, **10**, 1 (2019).
7. J. Chen, H. Zhang, H. Yang, J. Lei, A. Naveed, J. Yang, Y. Nuli, and J. Wang, *Energy Storage Mater.*, **27**, 307 (2020).
8. Y. Shen, J. Zhang, Y. Pu, H. Wang, B. Wang, J. Qian, Y. Cao, F. Zhong, X. Ai, and H. Yang, *ACS Energy Lett.*, **4**, 1717 (2019).
9. Y. Liu, A. K. Haridas, K. K. Cho, Y. Lee, and J. H. Ahn, *J. Phys. Chem. C*, **121**, 26172 (2017).
10. H. Yang, J. Chen, J. Yang, Y. Nuli, and J. Wang, *Energy Storage Mater.*, **31**, 187 (2020).
11. Y. Li, Q. Zeng, I. R. Gentle, and D. W. Wang, *J. Mater. Chem. A*, **5**, 5460 (2017).
12. Z. Wu, S. Bak, Z. Shadike, S. Yu, E. Hu, X. Xing, Y. Du, X. Yang, H. Liu, and P. Liu, *ACS Appl. Mater. Interfaces*, **13**, 31733 (2021).
13. M. H. Ryou et al., *Adv. Mater.*, **25**, 1571 (2013).
14. K. M. Abraham, *ACS Energy Lett.*, **5**, 3544 (2020).
15. H. Liu et al., *Mater. Today*, **42**, 17 (2021).
16. L. Wang, X. He, J. Li, M. Chen, J. Gao, and C. Jiang, *Electrochim. Acta*, **72**, 114 (2012).
17. J. Fanous, M. Wegner, J. Grimminger, Ä. Andresen, and M. R. Buchmeiser, *Chem. Mater.*, **23**, 5024 (2011).
18. S. Wei, L. Ma, K. E. Hendrickson, Z. Tu, and L. A. Archer, *J. Am. Chem. Soc.*, **137**, 12143 (2015).
19. E. Markevich, G. Salitra, F. Chesneau, M. Schmidt, and D. Aurbach, *ACS Energy Lett.*, **2**, 1321 (2017).
20. Y. Zhang, Y. Zhong, Q. Shi, S. Liang, and H. Wang, *J. Phys. Chem. C*, **122**, 21462 (2018).
21. M. He, L. X. Yuan, W. X. Zhang, X. L. Hu, and Y. H. Huang, *J. Phys. Chem. C*, **115**, 15703 (2011).